The Journal of Chemical Physics

Chemical and hydrodynamic alignment of an enzyme

Cite as: J. Chem. Phys. **150**, 115102 (2019); https://doi.org/10.1063/1.5081717
Submitted: 15 November 2018 . Accepted: 26 February 2019 . Published Online: 18 March 2019

T. Adeleke-Larodo, J. Agudo-Canalejo, and R. Golestanian

The Journal of Chemical Physics ARTICLE scitation.org/journal/jcp

Chemical and hydrodynamic alignment of an enzyme

Cite as: J. Chem. Phys. 150, 115102 (2019); doi: 10.1063/1.5081717
Submitted: 15 November 2018 • Accepted: 26 February 2019 •
Published Online: 18 March 2019 • Corrected: 20 March 2019

T. Adeleke-Larodo,[1,a)] J. Agudo-Canalejo,[1,2,b)] and R. Golestanian[1,3,c)]

AFFILIATIONS

[1]Rudolf Peierls Centre for Theoretical Physics, University of Oxford, Oxford OX1 3PU, United Kingdom
[2]Department of Chemistry, The Pennsylvania State University, University Park, Pennsylvania 16802, USA
[3]Max Planck Institute for Dynamics and Self-Organization (MPIDS), Am Fassberg 17, D-37077 Göttingen, Germany

Note: This article is part of the Special Topic "Chemical Physics of Active Matter" in J. Chem. Phys.
[a)]**Electronic mail:** tunrayo.adeleke-larodo@physics.ox.ac.uk.
[b)]**Electronic mail:** jaime.agudocanalejo@physics.ox.ac.uk.
[c)]**Electronic mail:** ramin.golestanian@ds.mpg.de

ABSTRACT

Motivated by the implications of the complex and dynamic modular geometry of an enzyme on its motion, we investigate the effect of combining long-range internal and external hydrodynamic interactions due to thermal fluctuations with short-range surface interactions. An asymmetric dumbbell consisting of two unequal subunits, in a nonuniform suspension of a solute with which it interacts via hydrodynamic interactions as well as non-contact surface interactions, is shown to have two alignment mechanisms due to the two types of interactions. In addition to alignment, the chemical gradient results in a drift velocity that is modified by hydrodynamic interactions between the constituents of the enzyme.

I. INTRODUCTION

While the role of enzymes in accelerating and regulating life-sustaining biochemical reactions inside cells is widely accepted, the mechanical response of an enzyme to the biochemical environment and its effect on how the enzyme functions has recently become a topic of interest because of the potential implications in understanding metabolic processes[1,2] and the possibility of exploiting enzyme functionalities to produce biocompatible micro- and nanoscale controllable machines.[3,4] In the context of self-propelled low-Reynolds number particles, propulsion due to phoretic effects has been studied extensively, theoretically and experimentally.[5] The question that is now being asked is whether enzyme molecules, undergoing catalytic turnover in varying reactant concentrations can exhibit similar effects.

A number of experiments have reported enhanced diffusion of an appreciable number of different enzymes in the presence of a homogeneous distribution of their substrate, with a Michaelis-Menten dependence of the diffusion coefficient on substrate concentration.[3,6–10] More recently, there have been experimental reports of directed motion of catalytically active enzymes when the substrate concentration is nonuniform so that there is a concentration gradient. The phenomenon has been observed for various enzymes and has typically been seen to cause movement towards the concentration gradient (reported in catalase and urease,[3,11] RNA polymerase,[6] DNA polymerase,[8] and hexokinase and aldolase[12]). The opposite has also been reported, where the enzymes (urease and acetylcholinesterase) are seen to move away from their substrate.[13] These observations are surprising because of the size of a single enzyme molecule and its implication on the necessary time-scale of such a dynamics. A perceivable response of an enzyme to a local gradient would be the culmination of overcoming thermal fluctuations and viscous effects that are expected to have significant effects on dynamics at the micro- and nanoscopic length scales and are amplified inside a cell. Several possible theories have been suggested that partially address the experimental observations.[14]

Initial theories to explain enhanced diffusion of enzymes relied on nonequilibrium aspects of the catalytic cycle.[9,15–18] We recently proposed an asymmetric dumbbell model for an enzyme to study the

diffusion of a single molecule.[19] With this model, we proposed an equilibrium mechanism for the phenomenon of enhanced diffusion of an enzyme in the presence of its substrate, or indeed any molecule that is able to occupy the binding site and induce conformational changes in the enzyme, such as an inhibitor. A natural question is to ask whether these effects are also relevant to the motion of an enzyme in the presence of concentration gradients of their substrate.

In this paper the specific geometry of an asymmetric dumbbell is adopted to study the response of the modular structure of an oligomeric enzyme to an externally imposed gradient of a chemical that interacts with the enzyme. We find that the presence of hydrodynamic and non-covalent interactions between the model enzyme and the chemical molecules leads to alignment of the enzyme driven by both types of interaction. In a fluid containing substrate with concentration ρ_s, the probability density $\tilde{\rho}_e(\boldsymbol{R}, \hat{\boldsymbol{n}}; t)$ of the model enzyme being located at position $\boldsymbol{R}$ with orientation $\hat{\boldsymbol{n}}$ evolves under the Smoluchowki equation

$$\begin{aligned}\partial_t \tilde{\rho}_e(\boldsymbol{R}, \hat{\boldsymbol{n}}; t) = {} & \nabla_{\boldsymbol{R}} \cdot [\boldsymbol{D}^t \cdot \nabla_{\boldsymbol{R}} \tilde{\rho}_e - (\boldsymbol{\mu}^v \cdot \nabla_{\boldsymbol{R}} \rho_s) \tilde{\rho}_e] \\ & + \boldsymbol{\mathcal{R}} \cdot [D^r \boldsymbol{\mathcal{R}} \tilde{\rho}_e - \mu^\omega (\hat{\boldsymbol{n}} \times \nabla_{\boldsymbol{R}} \rho_s) \tilde{\rho}_e] \\ & + \boldsymbol{\mathcal{R}} \cdot [\boldsymbol{D}^c \cdot \nabla_{\boldsymbol{R}} \tilde{\rho}_e] + \nabla_{\boldsymbol{R}} \cdot [(\boldsymbol{D}^c)^{\mathrm{T}} \cdot \boldsymbol{\mathcal{R}} \tilde{\rho}_e] \end{aligned} \quad (1)$$

in the absence of substrate binding, which is incorporated later.

The first line of Eq. (1) has a generic form, describing motion that is not specific to the dumbbell geometry: translational diffusion with diffusion coefficient $\boldsymbol{D}^t$ and diffusiophoretic drift with velocity $\mathbf{V}_{\mathrm{ph}} = \boldsymbol{\mu}^v \cdot \nabla_{\boldsymbol{R}} \rho_s$ due to non-covalent interactions of the substrate with the surface of the enzyme.[20,21] For the dumbbell, the phoretic mobility $\boldsymbol{\mu}^v$ is the sum of the phoretic mobilities of the individual subunits due to diffusiophoresis and a correction due to coupling of the subunits. The second line characterises the rotational motion of the enzyme: rotational diffusion of the orientation vector $\hat{\boldsymbol{n}}$ with diffusion coefficient D^r and a term corresponding to alignment of the orientation vector parallel or anti-parallel to the concentration gradient that is controlled by μ^ω. This alignment mechanism was previously known[22] and achieved by artificial symmetry breaking (by methods such as patterning the surface of a spherical particle with a substance that undergoes catalytic activity with the chemical in the bulk) here emerges naturally as a result of the in-built asymmetry of an enzyme. The final line of Eq. (1) contains contributions to the motion due to the asymmetric dumbbell geometry, where $\boldsymbol{D}^c$ is a tensor coupling translational and rotational motion of the subunits and $(\boldsymbol{D}^c)^{\mathrm{T}}$ is the transpose tensor. The first term gives a purely hydrodynamic contribution to alignment that comes from gradients in the density field.

In Ref. 23, it was shown that substrate binding results in an additional contribution to the drift velocity of an enzyme in a substrate concentration gradient, due to the difference in diffusion coefficient between the free and bound states of the enzyme. The same study also showed that the phoretic drift velocity, just like the diffusion coefficient,[10,19] has a Michaelis-Menten-like dependence on the substrate concentration. However, the latter study did not consider the modular structure of the enzyme. By including the effect of binding in Eq. (1), we will show that the evolution equation can be written in the form

$$\partial_t c_{\mathrm{tot}}(\boldsymbol{R}; t) = \nabla_{\boldsymbol{R}} \cdot \left\{ D^{\mathrm{eff}}(\boldsymbol{R}) \nabla_{\boldsymbol{R}} c_{\mathrm{tot}} - \left[\mathbf{V}^{\mathrm{eff}}_{\mathrm{ph}}(\boldsymbol{R}) + \mathbf{V}^{\mathrm{eff}}_{\mathrm{bi}}(\boldsymbol{R}) \right] c_{\mathrm{tot}} \right\}, \quad (2)$$

which has the same form as the one derived in Ref. 23, except that now the effective diffusion coefficient D^{eff} and the effective velocities $\mathbf{V}^{\mathrm{eff}}_{\mathrm{ph}}$ and $\mathbf{V}^{\mathrm{eff}}_{\mathrm{bi}}$ contain corrections due to fluctuations and hydrodynamic interactions between the subunits. We note that the derivation of Eq. (2) from Eq. (1) assumes that the mean time for formation of an enzyme-substrate complex is much greater than the rotational diffusion time of the enzyme (this could be an attribute of a specific enzyme, or because the solution is sufficiently dilute so that there is a long time between the enzyme's encounters with substrate molecules).

In Sec. II, we describe the system and present the main steps in our calculation for determining the alignment mechanisms for our model enzyme in an interacting chemical field. Specific details of the calculation are reserved for the supporting appendices. Following this, an effective mobility is derived for the long-time, large length-scale dynamics. The alignment of the enzyme due to diffusiophoresis is examined in more detail. In Sec. V, we consider the effect of the binding and unbinding of substrate molecules on the directed motion of our enzyme. Finally, we conclude with a discussion of the significance and possible implications of our results for further investigations into the dynamics of enzymes, and other low-Reynolds number modular structures for which internal hydrodynamics may play a role.

II. MODEL

For many enzymes, there is a separation of time scales between their dynamics and reactions that allows us to make simplifying approximations. Consider the following simple: the Michaelis-Menten model for enzyme catalysis, where substrate approaches the enzyme by a diffusive process E + S ⇆ ES ⇆ E + P. The characteristic time scales of the system are identified as the following: the mean binding time for the formation of an enzyme-substrate complex ES; the mean time for catalysis, when product is formed; the relaxation time of internal fluctuations of the enzyme; the translational and rotational diffusion times; and the relaxation time of the fluid around the enzyme.[24] Initially, the reactions of the enzyme are ignored with the understanding that the relaxation times for the internal dynamics, and the diffusion times for substrate molecules are much smaller. For most enzymes, the catalytic step is typically orders of magnitude slower than the diffusion of substrates and products.

Submerged in an inhomogeneous substrate concentration, we consider an asymmetric dumbbell consisting of two unequal subunits, taken to be rigid spheres to simplify the hydrodynamic treatment, which are subjected to thermal fluctuations that mediate hydrodynamic interactions between the subunits and between the subunits and substrate molecules in the bulk. In addition, there is an interaction potential between the subunits which sets a preferred separation between them, and controls the magnitude of the fluctuations around the equilibrium separation, i.e., the flexibility of the enzyme. A schematic of the setup is shown in Fig. 1. Each subunit has separate direct interactions with the substrate molecules in the bulk, which can be either attractive or repulsive; for example, coming from van der Waals, electrostatic or steric forces.

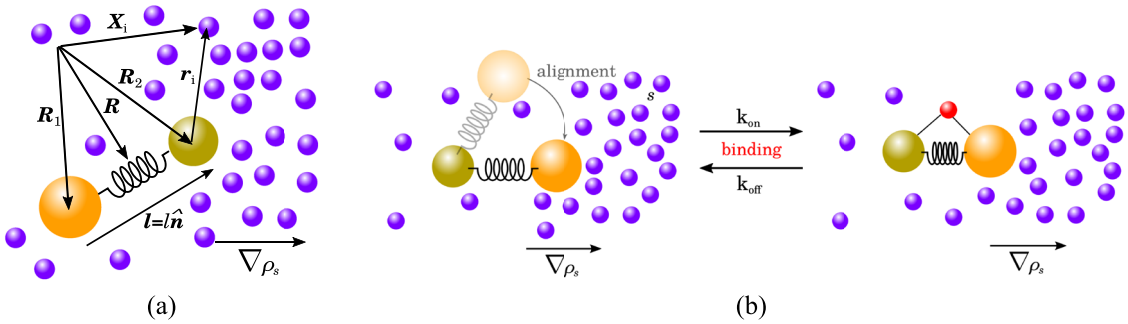

FIG. 1. (a) A free enzyme in a gradient of substrate molecules. The free enzyme interacts with substrate molecules in the bulk via pairwise hydrodynamic and non-covalent surface interactions. (b) Additionally, the free enzyme can bind to a substrate molecule to form a complex with rate k_{on} which decomposes at rate k_{off}.

III. SINGLE MOLECULE ALIGNMENT

The stochastic dynamics of the model enzyme, with subunits at positions $\boldsymbol{R}_1$ and $\boldsymbol{R}_2$, in an unbounded bath of N substrate molecules at positions $\boldsymbol{X}_1, \ldots, \boldsymbol{X}_N$, is characterised by the $(N+2)$-particle distribution $\rho(\boldsymbol{R}_1, \boldsymbol{R}_2, \boldsymbol{X}_1, \ldots, \boldsymbol{X}_N; t)$. We assume that the distribution evolves under the Smoluchowski equation

$$\begin{aligned}\partial_t\rho(\boldsymbol{R}_1,\boldsymbol{R}_2,\boldsymbol{X}_1,\ldots,\boldsymbol{X}_N;t) = &\sum_{i,j=1}^{2}\nabla_{\boldsymbol{R}_i}\cdot\left(\boldsymbol{\mu}^{ij}\cdot\left[k_\mathrm{B}T\nabla_{\boldsymbol{R}_j}\rho+(\nabla_{\boldsymbol{R}_j}\phi)\rho\right]\right)\\ &+\sum_{i=1}^{N}\Bigg\{\sum_{j=1}^{2}\Big[\nabla_{\boldsymbol{R}_j}\cdot\left(\boldsymbol{\mu}^{js}\cdot\left[k_\mathrm{B}T\nabla_{\boldsymbol{X}_i}\rho\right.\right.\\ &\left.+(\nabla_{\boldsymbol{X}_i}\phi)\rho\right]\Big)+\nabla_{\boldsymbol{X}_i}\cdot\left(\boldsymbol{\mu}^{sj}\cdot\left[k_\mathrm{B}T\nabla_{\boldsymbol{R}_j}\rho\right.\\ &\left.\left.+(\nabla_{\boldsymbol{R}_j}\phi)\rho\right]\right)\Big]+\nabla_{\boldsymbol{X}_i}\cdot\left(\boldsymbol{\mu}^{ss}\cdot\left[k_\mathrm{B}T\nabla_{\boldsymbol{X}_i}\rho\right.\right.\\ &\left.\left.+(\nabla_{\boldsymbol{X}_i}\phi)\rho\right]\right)\Bigg\}. \qquad (3)\end{aligned}$$

Here, the second line is the contribution from the isolated enzyme,[19] with self- and hydrodynamic mobility tensors $\boldsymbol{\mu}^{ij}$. The third and fourth lines are due to interactions between the subunits and substrate molecules, with hydrodynamic mobility tensors $\boldsymbol{\mu}^{js}$ and $\boldsymbol{\mu}^{sj}$. Finally, the fifth line is due to interactions between the N substrate molecules, with hydrodynamic mobility tensors $\boldsymbol{\mu}^{ss}$. The superscript s is used for the mobility tensors since substrate molecules are indistinguishable. Strictly, the mobility tensors as well as the interaction potential ϕ depend on the position of all $(N+2)$ particles. In a sufficiently dilute solution, where three-body and higher order interactions are rare, the interaction potential ϕ can be approximated as the sum of pair potentials between the dumbbell subunits and the pair potentials between each subunit and a substrate molecule, $\phi(\boldsymbol{R}_1,\boldsymbol{R}_2,\boldsymbol{X}_1,\ldots,\boldsymbol{X}_N) = \phi^\mathrm{e}(\boldsymbol{R}_1,\boldsymbol{R}_2) + \sum_{j=1}^{2}\sum_{i=1}^{N}\phi^{js}(\boldsymbol{R}_j,\boldsymbol{X}_i)$. In addition, if the substrate molecules are small, we can assume that the subunit self-mobilities μ^{ii} are constant, and for $i \neq j$, the cross-mobilities μ^{ij} contain only the pair interactions. In its current form, Eq. (3) holds information on the evolution of the model enzyme as well as the N substrate molecules. Since we are only interested in the evolution of the enzyme, we define the two-particle distribution

$$\rho_\mathrm{e}(\boldsymbol{R}_1,\boldsymbol{R}_2;t) = \int \mathrm{d}\boldsymbol{X}_1,\ldots,\mathrm{d}\boldsymbol{X}_N\,\rho(\boldsymbol{R}_1,\boldsymbol{R}_2,\boldsymbol{X}_1,\ldots,\boldsymbol{X}_N;t). \qquad (4)$$

The evolution equation for the two-particle distribution is not closed as it retains information of higher order interactions through the three-particle distribution $\rho_\mathrm{es}(\boldsymbol{R}_1, \boldsymbol{R}_2, \boldsymbol{X}; t)$. This is the first of the Bogoliubov-Born-Green-Kirkwood-Yvon-type (BBGKY) hierarchies we will face. Here, the evolution of ρ_e and ρ_es are coupled through solvent-mediated hydrodynamic interactions and the interaction potential ϕ^{js}. For a dilute solution (again this amounts to neglecting three-body interactions), and considering that solute molecules are much smaller than the enzyme and thus the solute concentration field relaxes quickly, a natural closure approximation is

$$\rho_\mathrm{es}(\boldsymbol{R}_1,\boldsymbol{R}_2,\boldsymbol{X};t) \simeq \rho_\mathrm{e}(\boldsymbol{R}_1,\boldsymbol{R}_2)\frac{\rho_\mathrm{s}(\boldsymbol{X};t)}{N}\mathrm{e}^{-\frac{\phi^{1s}+\phi^{2s}}{k_\mathrm{B}T}}. \qquad (5)$$

A second approximation is needed in order to be able to write the remaining integral over the substrate position into a manifestly phoretic form. In Eq. (5), there is still a coupling of the interactions ϕ^{1s} and ϕ^{2s} between the subunits and the substrate molecules through the Boltzmann weight. We assume that the range of the pair potentials is much shorter than the typical distance between subunits 1 and 2, that is, that the two potentials do not overlap, implying that a substrate molecule never "feels" both subunits at the same time. The evolution equation for the two-particle distribution (4) can then be written as

$$\begin{aligned}\partial_t\rho_\mathrm{e}(\boldsymbol{R}_1,\boldsymbol{R}_2;t) = &\sum_{i,j=1}^{2}\Bigg\{\nabla_{\boldsymbol{R}_i}\cdot\left(\boldsymbol{\mu}^{ij}\cdot\left[k_\mathrm{B}T\nabla_{\boldsymbol{R}_j}\rho_\mathrm{e}+(\nabla_{\boldsymbol{R}_j}\phi^\mathrm{e})\rho_\mathrm{e}\right]\right)\\ &+\nabla_{\boldsymbol{R}_i}\cdot\left[k_\mathrm{B}T\rho_\mathrm{e}\int_{\boldsymbol{X}}(\boldsymbol{\mu}^{is}-\boldsymbol{\mu}^{ij})(\mathrm{e}^{-\frac{\phi^{js}}{k_\mathrm{B}T}}-1)\nabla_{\boldsymbol{X}}\rho_\mathrm{s}\right]\Bigg\}. \qquad (6)\end{aligned}$$

Alone, the second line describes the evolution of the enzyme in a fluid in the absence of a substrate concentration gradient.[19] The third line corresponds to phoretic response to the chemical field: for $i = j$ it describes diffusiophoresis of a single particle,[20,23] whereas for $i \neq j$, the term is new and unique to the case of a dumbbell, given that it mixes the direct interactions between the substrate particles and the j particle with the hydrodynamic interactions between substrate

and the i particle, and the hydrodynamic interactions between i and j (i.e., 1 and 2).

We evaluate the integral in (6) representing the phoretic response of the enzyme by assuming that the substrate particles are point-like, that the interaction ϕ^{js} is very short-ranged, and that the concentration ρ_s in the proximity of a subunit is the solution to the Laplace equation with no flux boundary conditions at the surface of the subunit when there is a uniform gradient $\nabla\rho_s^\infty$ at infinity. The details of the calculation are given in Appendix A. To the order considered, the integrals corresponding to single-particle phoresis have additional contributions which come from solving for the substrate concentration field in the presence of both subunits simultaneously (see Appendix A 3). Introducing the results for the integration of the phoretic terms into (6) and defining the centre and elongation coordinates of the dumbbell, $\boldsymbol{R} = (\boldsymbol{R}_1 + \boldsymbol{R}_2)/2$ and $\boldsymbol{l} = \boldsymbol{R}_2 - \boldsymbol{R}_1$, with $\boldsymbol{l} = l\hat{\boldsymbol{n}}$, the Smoluchowski equation can be rewritten as

$$\begin{aligned}\partial_t\rho_e(\boldsymbol{R},\boldsymbol{l};t) = &+\frac{1}{2}\nabla_{\boldsymbol{R}}\cdot\left[\frac{1}{2}\mathbf{M}\cdot k_BT\nabla_{\boldsymbol{R}}\rho_e + \boldsymbol{\Gamma}\cdot\left(k_BT\nabla_{\boldsymbol{l}}\rho_e + (\nabla_{\boldsymbol{l}}U)\rho_e\right)\right]\\ &+\nabla_{\boldsymbol{l}}\cdot\left[\mathbf{W}\cdot\left(k_BT\nabla_{\boldsymbol{l}}\rho_e + (\nabla_{\boldsymbol{l}}U)\rho_e\right) + \frac{1}{2}\boldsymbol{\Gamma}\cdot k_BT\nabla_{\boldsymbol{R}}\rho_e\right]\\ &-\nabla_{\boldsymbol{R}}\cdot\left\{\rho_e\frac{\boldsymbol{\sigma}_1+\boldsymbol{\sigma}_2}{2}\cdot\nabla_{\boldsymbol{R}}\rho_s^\infty\right\}\\ &-\nabla_{\boldsymbol{l}}\cdot\left\{\rho_e(\boldsymbol{\sigma}_2-\boldsymbol{\sigma}_1)\cdot\nabla_{\boldsymbol{R}}\rho_s^\infty\right\},\end{aligned} \tag{7}$$

where the translation, rotation, and coupling tensors are defined, respectively, as the following linear combinations of the hydrodynamic mobility tensors

$$\begin{aligned}\mathbf{M} &= \boldsymbol{\mu}^{11} + \boldsymbol{\mu}^{22} + 2\boldsymbol{\mu}^{12},\\ \mathbf{W} &= \boldsymbol{\mu}^{11} + \boldsymbol{\mu}^{22} - 2\boldsymbol{\mu}^{12},\\ \boldsymbol{\Gamma} &= \boldsymbol{\mu}^{22} - \boldsymbol{\mu}^{11}.\end{aligned} \tag{8}$$

We have also performed the relabelling $\phi^e(\boldsymbol{R}_1, \boldsymbol{R}_2) = U(l)$ and have defined

$$\boldsymbol{\sigma}_1 \equiv \frac{k_BT}{\eta}\left\{A_1\mathbf{1} + \frac{a_2^3}{l^3}\left(B_2 - \frac{3}{2}A_1\right)\left(\hat{\boldsymbol{n}}\hat{\boldsymbol{n}} - \frac{\mathbf{1}}{3}\right)\right\} \tag{9}$$

and

$$\boldsymbol{\sigma}_2 \equiv \frac{k_BT}{\eta}\left\{A_2\mathbf{1} + \frac{a_1^3}{l^3}\left(B_1 - \frac{3}{2}A_2\right)\left(\hat{\boldsymbol{n}}\hat{\boldsymbol{n}} - \frac{\mathbf{1}}{3}\right)\right\}, \tag{10}$$

which are the phoretic mobility tensors of subunits 1 and 2, respectively. In each of them, the first term corresponds to the mobility of the isolated subunit, whereas the second term is a correction due to the presence of the other subunit (decaying as $1/l^3$). The a_i are the radii of the subunits and A_i and B_i are related to the values of the $\boldsymbol{X}$ integrals in (6) for $i = j$ and $i \neq j$, respectively; see Eqs. (A9)–(A10) and (A16)–(A17). For very short-ranged interactions, we can use $r_i = a_i + \delta$ with $\delta \ll a_i$ for the distance between subunit i and the substrate molecule at position $\boldsymbol{X}$, giving to the lowest order

$$A_i \approx \int_0^\infty \mathrm{d}\delta\delta(\mathrm{e}^{-\frac{\phi^{is}(\delta)}{k_BT}} - 1) \equiv \lambda_i^2, \tag{11}$$

where λ_i is the Derjaguin length[20,25,26] and

$$B_i \approx \frac{a_i}{10}\int_0^\infty \mathrm{d}\delta\,(\mathrm{e}^{-\frac{\phi^{is}(\delta)}{k_BT}} - 1) \equiv \frac{a_i}{10}\gamma_i, \tag{12}$$

where we have defined γ_i, which is a length scale of the order of the interaction range, but distinct from the Derjaguin length. It is equivalent to Anderson's *adsorption length*, which represents the amount of substrate adsorbed, per area of surface, divided by the bulk concentration at equilibrium.[20] Comparison of (11) and (12) shows that generally we should expect $B_i \gg A_i$, given that A_i is of the order of the interaction range squared, whereas B_i is of the order of the particle size times the interaction range. Typically the Derjaguin length is of the order of a few angstroms[20] and the hydrodynamic radius of an enzyme is of the order of nm, about 7 nm for urease.[7]

Equation (7) describes the probabilistic evolution in the complete phase space of a single enzyme, at a time that is less than the mean association time for the formation of an enzyme-substrate complex. This is a consequence of the assumption that the solution is dilute. However, it still retains information of the slow ($\boldsymbol{R}$) and fast ($\boldsymbol{l}$) dynamics. The fast dynamics is composed of fluctuations around the equilibrium separation of the subunits that affect the conformations of the enzyme, and diffusion of the orientation vector $\hat{\boldsymbol{n}}$. Equation (7) is simplified by a reduction of the phase space to include only the relevant degrees of freedom, here, $\hat{\boldsymbol{n}}$ and $\boldsymbol{R}$ (see Appendix B). The relaxation time for vibrations in l is smaller than the rotational diffusion time because the ratio between them is the relative deformation of the enzyme due to thermal fluctuations, and is thus less than one.[19] The dependence on l is therefore eliminated by considering sufficiently large times. Explicitly, we assume that the l-dependence of ρ_e is Boltzmann-like and define the separation-averaged two-particle distribution $\tilde{\rho}_e = \int \mathrm{d}l\, l^2\rho_e$ and the average of a function that depends on the subunit separation $\langle f\rangle = \frac{1}{\tilde{\rho}_e}\int \mathrm{d}l\, l^2 f\,(l)\,\rho_e$. Averaging Eq. (7) in this way, while treating the orientation as a constant, we arrive at Eq. (1) with translational diffusion tensor

$$\boldsymbol{D}^t \equiv \frac{1}{4}k_BT\langle\mathbf{M}\rangle, \tag{13}$$

rotational diffusion coefficient

$$D^r \equiv k_BT\left\langle\frac{W_I}{l^2}\right\rangle, \tag{14}$$

translation-rotation coupling tensor

$$[\boldsymbol{D}^c]_{ij} \equiv \frac{k_BT}{2}\left\langle\frac{\Gamma_I}{l}\right\rangle\epsilon_{ikj}\hat{n}_k, \tag{15}$$

with transpose $(\boldsymbol{D}^c)^{\mathrm{T}}$, satisfying $(\boldsymbol{D}^c)^{\mathrm{T}} = -\boldsymbol{D}^c$, phoretic mobility tensor

$$\begin{aligned}\boldsymbol{\mu}^{\mathrm{v}} \equiv \frac{k_BT}{2\eta}\Bigg[&(A_1+A_2)\mathbf{1} + \left\langle\frac{1}{l^3}\right\rangle\left(a_1^3B_1 + a_2^3B_2 - \frac{3}{2}(a_2^3A_1 + a_1^3A_2)\right)\\ &\times\left(\hat{\boldsymbol{n}}\hat{\boldsymbol{n}} - \frac{\mathbf{1}}{3}\right)\Bigg]\end{aligned} \tag{16}$$

$$= \left[\mu_I^{\mathrm{v}}\mathbf{1} + \mu_D^{\mathrm{v}}\hat{\boldsymbol{n}}\hat{\boldsymbol{n}}\right] \tag{17}$$

and the response of the orientation vector of the dumbbell to the local chemical gradient

$$\mu^{\omega} \equiv \frac{k_B T}{\eta}\left[\left\langle\frac{1}{l}\right\rangle(A_2 - A_1) + \frac{1}{3}\left\langle\frac{1}{l^4}\right\rangle \times\left(a_2^3 B_2 - a_1^3 B_1 + \frac{3}{2}(a_1^3 A_2 - a_2^3 A_1)\right)\right]. \tag{18}$$

From Eq. (17), we see that the translational drift velocity comes from two distinct responses to the substrate field: diffusiophoresis of the enzyme along the substrate concentration gradient, which is controlled by μ_I^{v} and an anisotropic response instantaneously along $\hat{\boldsymbol{n}}$, which is controlled by μ_D^{v}, which leads to an average drift along the gradient after a time that is larger than the rotational diffusion time. The two mechanisms have been described for active colloids, where the control parameters of the response to the chemical gradient are determined by the surface patterning of the colloid and have both passive and active contributions.[22]

The angular velocity of the enzyme will turn it towards or away from the chemical field, depending on the value of μ^{ω}, and hence the sign of the interactions ϕ^{is}. This parameter will later be discussed in greater detail.

A. Polarisation

We define the global density $c(\boldsymbol{R};t) = \int \mathrm{d}\hat{\boldsymbol{n}}\,\tilde{\rho}_{\mathrm{e}}$ and polar order parameter $\boldsymbol{p}(\boldsymbol{R};t) = \int \mathrm{d}\hat{\boldsymbol{n}}\,\hat{\boldsymbol{n}}\tilde{\rho}_{\mathrm{e}}$ of the enzyme, which are the relevant quantities in the large time limit if we assume that rotational diffusion is fast. The equation for the polar order parameter is the first moment of Eq. (1). However, the equation for $\boldsymbol{p}$ is coupled to higher order moments of the distribution in another BBGKY hierarchy. The usual protocol for truncating such a hierarchy is to assume that $\boldsymbol{p}$ is constant over sufficiently large distances and that it relaxes quickly. Additionally, that the orientation decorrelates after a sufficiently long time so that we can set $\boldsymbol{Q}(\boldsymbol{R};t) = \int \mathrm{d}\hat{\boldsymbol{n}}\left(\hat{\boldsymbol{n}}\hat{\boldsymbol{n}} - \frac{1}{3}\right)\tilde{\rho}_{\mathrm{e}}$ and higher order moments to zero. With these approximations, we find the following expression for the polar order parameter

$$\boldsymbol{p} = \frac{1}{3D^r}\left[-D^c \nabla_{\boldsymbol{R}} c + \mu^{\omega}(\nabla_{\boldsymbol{R}}\rho_{\mathrm{s}}^{\infty})c\right]. \tag{19}$$

This expression has two terms, corresponding to two mechanisms by which a modular enzyme can be polarised. The first term corresponds to a purely hydrodynamic mechanism which is controlled by the translation-rotation coupling scalar $D^c = \frac{k_B T}{2}\left\langle\frac{\Gamma_I}{l}\right\rangle$, which tends to align the enzyme with the gradient in the *enzyme* concentration field $\nabla_{\boldsymbol{R}} c$, so that the smaller subunit is in the lower concentration region and the larger subunit in the higher concentration region (this is because D^c is positive or negative when subunit 2 is smaller or larger than subunit 1, respectively). The second term corresponds to a phoretic mechanism which aligns the enzyme with the gradient in the *substrate* concentration field $\nabla_{\boldsymbol{R}}\rho_{\mathrm{s}}^{\infty}$, with positive and negative values of μ^{ω} resulting in subunit 2 being in the region of higher or lower substrate concentration, respectively. We note that, to lowest order, the sign of μ^{ω} is controlled by the sign of $(A_2 - A_1)$, which leads to the intuitive result that subunit 2 is in the region of higher substrate concentration when $A_2 > A_1$ (i.e., when subunit 2 undergoes a stronger phoretic attraction towards the substrate than subunit 1), and vice versa when $A_1 > A_2$. In the special case in which the two subunits interact identically with the substrate ($A_1 = A_2 = A$ and $B_1 = B_2 = B$), the sign of μ^{ω} is controlled by the sign of the higher order corrections $(a_2^3 - a_1^3)(B - \frac{3}{2}A)$. Because in general we expect B to be much larger so that $B - \frac{3}{2}A \approx B$, the enzyme will align so that the largest subunit is in the region of higher or lower substrate concentration if the interactions are attractive ($B > 0$) or repulsive ($B < 0$), respectively. Beyond the closure approximation used here, we expect a non-linear coupling of the two alignment mechanisms.

IV. EFFECTIVE MOBILITY

Substituting the first moment of Eq. (1) into the zeroth moment and using the moment closure scheme described above to truncate the hierarchy, we derive a diffusion equation $\partial_t c(\boldsymbol{R};t) = D^{\mathrm{eff}}\nabla_{\boldsymbol{R}}^2 c - \mu^{\mathrm{eff}}\nabla_{\boldsymbol{R}}\cdot[(\nabla_{\boldsymbol{R}}\rho_{\mathrm{s}}^{\infty})c]$, with effective diffusion coefficient and phoretic mobility

$$D^{\mathrm{eff}} = D_{\mathrm{ave}}^t - \frac{2(D^c)^2}{3D^r} \tag{20}$$

and

$$\mu^{\mathrm{eff}} = \frac{k_B T}{\eta}\frac{(A_1 + A_2)}{2} - \frac{k_B T}{3\eta}\frac{\langle\Gamma_I/l\rangle}{\langle W_I/l^2\rangle}\left[\left\langle\frac{1}{l}\right\rangle(A_2 - A_1) + \frac{1}{3}\left\langle\frac{1}{l^4}\right\rangle\left(a_2^3 B_2 - a_1^3 B_1 + \frac{3}{2}\left(a_1^3 A_2 - a_2^3 A_1\right)\right)\right] = \mu_I^{\mathrm{v}} + \frac{1}{3}\mu_D^{\mathrm{v}} - \frac{2D^c}{3D^r}\mu^{\omega}. \tag{21}$$

The effective diffusion coefficient is as in Ref. 19, where D_{ave}^t is the average of the translational motion and there is a negative correction due to hydrodynamic coupling of the subunits of the enzyme. Similarly, we now find that the effective phoretic mobility is the average of the Anderson-type contribution to the diffusiophoresis of each subunit,[20] plus a correction that is due to intramolecular hydrodynamic interactions. The correction will typically have (to lowest order $\langle 1/l\rangle$) the same sign as $(A_L - A_S)$, where the subscripts L and S indicate the larger and smaller subunit, respectively.

Defining the average mobility $\tilde{\mu} = k_B T(A_1 + A_2)/2\eta$, the difference between the effective mobility of two interacting subunits and the average mobility of two non-interacting subunits is given by

$$\frac{\mu_{\mathrm{eff}} - \tilde{\mu}}{\tilde{\mu}} = -\frac{4D^c}{3D^r(1 + \tilde{A})}\left\{(\tilde{A} - 1)\left\langle\frac{1}{l}\right\rangle + \frac{a_1^3}{3}\left\langle\frac{1}{l^4}\right\rangle\left[\alpha\left(\zeta^3\tilde{A} - 1\right) + \frac{3}{2}\left(\tilde{A} - \zeta^3\right)\right]\right\}, \tag{22}$$

with $\tilde{A} = A_2/A_1$, $\zeta = a_2/a_1$, and where we have taken for simplicity $B_i = \alpha A_i$ with the same proportionality constant for both subunits. From Eqs. (11) and (12), α is of the order of the particle size a_i divided by the interaction length λ_i, about an order of magnitude for nm size enzymes and angstrom Derjaguin length, and we thus use $\alpha \approx 10$ in all figures in the following.

In Fig. 2 we have plotted the corrections to the average mobility as given by (22) as a function of the relative fluctuations of the enzyme, for some selected values of the relative phoretic

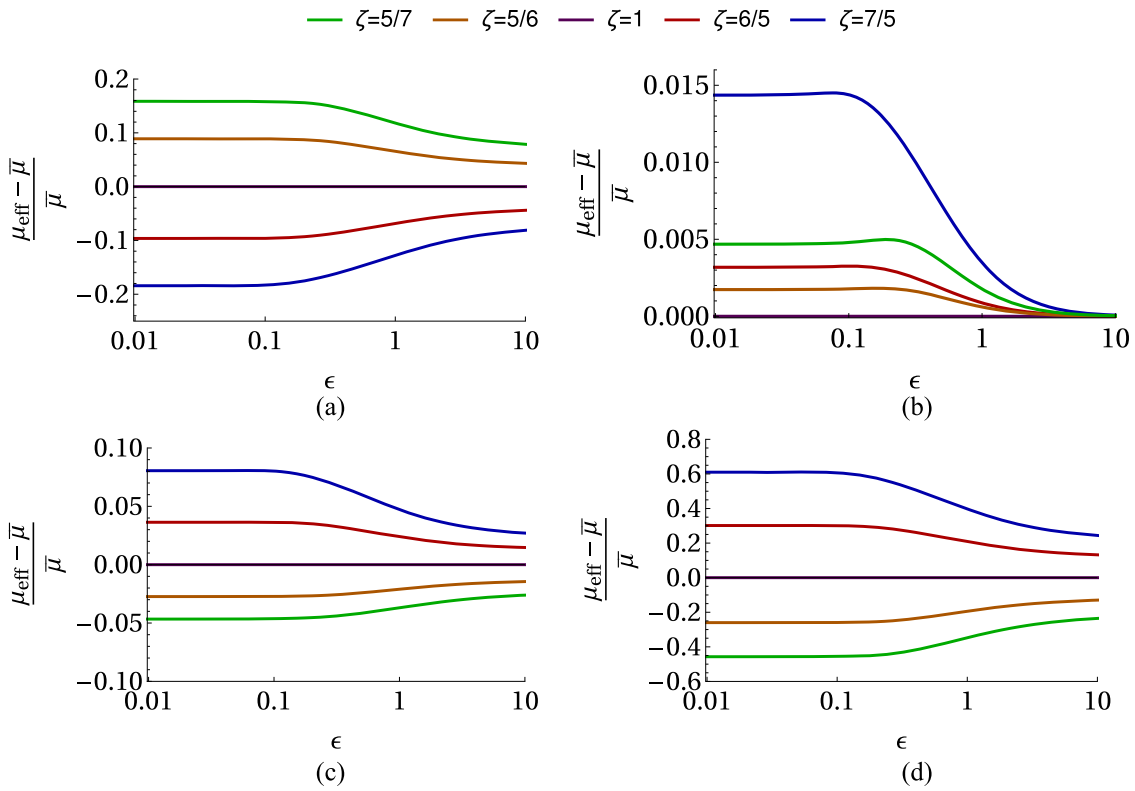

FIG. 2. $(\mu_{\text{eff}} - \bar{\mu})/\bar{\mu}$ from Eq. (22) for subunits interacting via a harmonic potential with stiffness k as a function of the fluctuation parameter $\epsilon = \sqrt{k_B T/ka^2}$, where a is the typical size of the dumbbell. The lines represent different values of the ratio between the subunit sizes ζ, and the ratio $a_1/a = 0.3$ is constant in all plots. The Oseen mobility functions have been used for all plots. In (a) $\tilde{A} = 0$, (b) $\tilde{A} = 1$, (c) $\tilde{A} = 2$, and (d) $\tilde{A} = -2$.

mobility of the subunits, $\tilde{A}$, and the relative size of the subunits, ζ. For $\zeta = 1$ (i.e., subunits of equal size), there is no change in mobility for interacting subunits in any case. For $\tilde{A} = 0$ (see Fig. 2(a)) when the interaction of subunit 2 with the substrate is negligible, the effective mobility is reduced if subunit 2 is larger than subunit 1 ($\zeta > 1$), and enhanced if subunit 2 is smaller ($\zeta < 1$). For $\tilde{A} = 1$ (see Fig. 2(b)) when the interactions of the two subunits with the substrate are equal, the corrections are smaller (the correction of order $\langle 1/l \rangle$ vanishes and only the correction of order $\langle 1/l^4 \rangle$ survives) but they always enhance the effective mobility of the dumbbell, independently of whether subunit 2 is larger or smaller than subunit 1. For $\tilde{A} = 2$ and $\tilde{A} = -2$ [see Figs. 2(c) and 2(d)], when the interactions of the subunit 2 with the substrate dominate over the interactions of subunit 1 with the substrate (no matter the sign, i.e., $|\tilde{A}| > 1$), the effective mobility is reduced if subunit 2 is smaller than subunit 1 ($\zeta < 1$) and enhanced if subunit 2 is larger ($\zeta > 1$). Generally, the absolute change in mobility is a decreasing function of the relative fluctuations of the dumbbell. We note that, in the previous sentences, "reduced" and "enhanced" refer to the *magnitude* of the mobility independently of its sign, i.e., reduction and enhancement of a negative average mobility imply making its value less and more negative, respectively.

If the two subunits have balancing mobilities ($A_2 = -A_1$, where we choose $A_1 > 0$ without loss of generality), the average mobility is zero ($\bar{\mu} = 0$) and the relative correction as in Eq. (22) is ill-defined. We can instead define the dimensionless quantity

$$\frac{\mu_{\text{eff}}}{\mu_1} = \frac{2D^c}{3D^r}\left[2\left\langle\frac{1}{l}\right\rangle + \frac{a_1^3}{3}\left\langle\frac{1}{l^4}\right\rangle\left(\alpha + \frac{3}{2}\right)\left(1 + \zeta^3\right)\right], \tag{23}$$

where $\mu_1 = k_B T A_1/\eta$ is the mobility of subunit 1 in isolation (which is opposite to the mobility of subunit 2, i.e., $\mu_1 = -\mu_2$). In Fig. 3 we

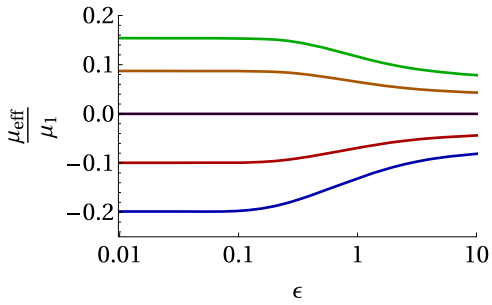

FIG. 3. μ_{eff}/μ_1 from Eq. (23) for subunits with balancing mobilities $A_2 = -A_1$ and $A_1 > 0$, interacting via a harmonic potential as a function of the dimensionless fluctuation parameter $\epsilon = \sqrt{k_B T/ka^2}$. The effective mobility vanishes for subunits of equal size, and its sign is determined by the sign of the mobility of the larger subunit.

have plotted (23) as a function of the relative fluctuations of the enzyme. The sign is controlled by that of D^c, which is positive if subunit 1 is larger than subunit 2, and negative if subunit 2 is larger than subunit 1. The sign of the effective mobility is thus governed by that of the mobility of the largest subunit. Moreover, if the subunits have equal size the effective mobility vanishes, as expected from symmetry.

V. ENZYME KINETICS

The results from Sec. IV can be extended to include a simplified kinetics for the enzyme. Enzymatic activity is considered as a two-state dynamical process with binding and unbinding of a substrate molecule to the enzyme binding site, but excluding the catalytic step in which the substrate is converted into product. The justification is that catalysis is typically much slower than the rate of binding activity. By introducing binding and unbinding, we find that the transport properties of the enzyme, which for a nonmodular enzyme were predicted to inherit a space dependence and the Michaelis-Menten kinetics of the mechanochemical cycle[23] are now subject to fluctuation-induced contributions in a generic way due to the non-vanishing coupling of translational and rotational modes of the dumbbell subunits. The derivation of the effective diffusion coefficient and drift velocities presented in this section follows what is presented in Ref. 23, where an enzyme was modelled as single particle.

Assuming that the rotational diffusion time of the enzyme is faster than the mean binding time (which is typically the case for most enzymes), at a time of the order of the mean binding time, the enzyme can be either free or bound to a substrate. If $\mathrm{S_{on}}(\boldsymbol{R}, \boldsymbol{X})$ is the probability that an enzyme at position $\boldsymbol{R}$ binds to a substrate molecule at position $\boldsymbol{X}$ to form a complex at $\boldsymbol{R}$ and $\mathrm{S_{off}}(\boldsymbol{R}, \boldsymbol{X})$ is the probability that the complex at $\boldsymbol{R}$ decomposes into a free enzyme at position $\boldsymbol{R}$ and a substrate molecule at $\boldsymbol{X}$, the densities of the two states obey the following equations:

$$\partial_t c_\mathrm{f}(\boldsymbol{R};t) = \nabla_{\boldsymbol{R}}\cdot\left[D_\mathrm{f}^{\mathrm{eff}}\nabla_{\boldsymbol{R}}c_\mathrm{f} - \mu_\mathrm{f}^{\mathrm{eff}}(\nabla_{\boldsymbol{R}}\rho_\mathrm{s}^{\infty})c_\mathrm{f}\right] - c_\mathrm{f}\int_{\boldsymbol{X}}\mathrm{S_{on}}(\boldsymbol{R},\boldsymbol{X})\rho_\mathrm{s}(\boldsymbol{X})\mathrm{e}^{-\frac{\phi_f^{1s}+\phi_f^{2s}}{k_\mathrm{B}T}} + c_\mathrm{b}\int_{\boldsymbol{X}}\mathrm{S_{off}}(\boldsymbol{R},\boldsymbol{X}) \quad (24)$$

and

$$\partial_t c_\mathrm{b}(\boldsymbol{R};t) = \nabla_{\boldsymbol{R}}\cdot\left[D_\mathrm{b}^{\mathrm{eff}}\nabla_{\boldsymbol{R}}c_\mathrm{b} - \mu_\mathrm{b}^{\mathrm{eff}}(\nabla_{\boldsymbol{R}}\rho_\mathrm{s}^{\infty})c_\mathrm{b}\right] + c_\mathrm{f}\int_{\boldsymbol{X}}\mathrm{S_{on}}(\boldsymbol{R},\boldsymbol{X})\rho_\mathrm{s}(\boldsymbol{X})\mathrm{e}^{-\frac{\phi_b^{1s}+\phi_b^{2s}}{k_\mathrm{B}T}} - c_\mathrm{b}\int_{\boldsymbol{X}}\mathrm{S_{off}}(\boldsymbol{R},\boldsymbol{X}), \quad (25)$$

where $c_\mathrm{f}(\boldsymbol{R};t) = \int \mathrm{d}\hat{\boldsymbol{n}}\,\tilde{\rho}_\mathrm{f}$ and $c_\mathrm{b}(\boldsymbol{R};t) = \int \mathrm{d}\hat{\boldsymbol{n}}\,\tilde{\rho}_\mathrm{b}$ are the free and bound state densities, respectively. The integrals over the substrate position $\boldsymbol{X}$ can be performed by invoking the approximation of very short-ranged interactions to choose $\mathrm{S_{on}}(\boldsymbol{R}, \boldsymbol{X}) = k_\mathrm{on}\delta(\boldsymbol{R}-\boldsymbol{X})$ and $\mathrm{S_{off}}(\boldsymbol{R}, \boldsymbol{X}) = k_\mathrm{off}\delta(\boldsymbol{R}-\boldsymbol{X})$, where k_on and k_off are the association and dissociation rates. After redefining k_on to include the constant $\exp\left[-(\phi_f^{1s}(0)+\phi_f^{2s}(0))/k_\mathrm{B}T\right]$, (24) and (25) become

$$\partial_t c_\mathrm{f}(\boldsymbol{R};t) = \nabla_{\boldsymbol{R}}\cdot\left[D_\mathrm{f}^{\mathrm{eff}}\cdot\nabla_{\boldsymbol{R}}c_\mathrm{f} - \mu_\mathrm{f}^{\mathrm{eff}}(\nabla_{\boldsymbol{R}}\rho_\mathrm{s}^{\infty})c_\mathrm{f}\right] - k_\mathrm{on}\rho_\mathrm{s}(\boldsymbol{R})c_\mathrm{f} + k_\mathrm{off}c_\mathrm{b} \quad (26)$$

and

$$\partial_t c_\mathrm{b}(\boldsymbol{R};t) = \nabla_{\boldsymbol{R}}\cdot\left[D_\mathrm{b}^{\mathrm{eff}}\cdot\nabla_{\boldsymbol{R}}c_\mathrm{b} - \mu_\mathrm{b}^{\mathrm{eff}}(\nabla_{\boldsymbol{R}}\rho_\mathrm{s}^{\infty})c_\mathrm{b}\right] + k_\mathrm{on}\rho_\mathrm{s}(\boldsymbol{R})c_\mathrm{f} - k_\mathrm{off}c_\mathrm{b}. \quad (27)$$

The experimentally relevant quantity is the total enzyme concentration

$$c_\mathrm{tot}(\boldsymbol{R};t) = c_\mathrm{f}(\boldsymbol{R};t) + c_\mathrm{b}(\boldsymbol{R};t) \quad (28)$$

because in the experimental set-up the free enzyme is indistinguishable from the enzyme-substrate complex. Furthermore, we can assume that binding is at local and instantaneous equilibrium since the time for motion in $\boldsymbol{R}$ is much greater than the binding time. This gives

$$k_\mathrm{on}c_\mathrm{f}(\boldsymbol{R};t)\rho_\mathrm{s}(\boldsymbol{R};t) \approx k_\mathrm{off}c_\mathrm{b}(\boldsymbol{R};t) \quad (29)$$

and, together with Eq. (28), we find

$$c_\mathrm{f} = \frac{K}{K+\rho_\mathrm{s}}c_\mathrm{tot} \qquad c_\mathrm{b} = \frac{\rho_\mathrm{s}}{K+\rho_\mathrm{s}}c_\mathrm{tot}. \quad (30)$$

Finally, the sum of (26) and (27) using (30) gives Eq. (2) for the total enzyme concentration, where the effective diffusion coefficient and phoretic velocity are averaged over the two states with a Michaelis-Menten weight

$$D^{\mathrm{eff}}(\boldsymbol{R}) = D_\mathrm{f}^{\mathrm{eff}} + (D_\mathrm{b}^{\mathrm{eff}} - D_\mathrm{f}^{\mathrm{eff}})\frac{\rho_\mathrm{s}(\boldsymbol{R})}{K+\rho_\mathrm{s}(\boldsymbol{R})}, \quad (31)$$

$$\mathbf{V}_{\mathrm{ph}}^{\mathrm{eff}}(\boldsymbol{R}) = \mathbf{V}_\mathrm{f}^{\mathrm{eff}}(\boldsymbol{R}) + [\mathbf{V}_\mathrm{b}^{\mathrm{eff}}(\boldsymbol{R}) - \mathbf{V}_\mathrm{f}^{\mathrm{eff}}(\boldsymbol{R})]\frac{\rho_\mathrm{s}(\boldsymbol{R})}{K+\rho_\mathrm{s}(\boldsymbol{R})}, \quad (32)$$

and a binding-induced contribution to the drift velocity arises due to the changes in diffusion coefficient of the enzyme between the free and bound states[23]

$$\mathbf{V}_{\mathrm{bi}}^{\mathrm{eff}}(\boldsymbol{R}) = -(D_\mathrm{b}^{\mathrm{eff}} - D_\mathrm{f}^{\mathrm{eff}})\nabla_{\boldsymbol{R}}\left(\frac{\rho_\mathrm{s}(\boldsymbol{R})}{K+\rho_\mathrm{s}(\boldsymbol{R})}\right). \quad (33)$$

In the equations above, $D_{\mathrm{f,b}}^{\mathrm{eff}}$ is given by (20) and $\mathbf{V}_{\mathrm{f,b}}^{\mathrm{eff}}(\boldsymbol{R}) = \mu_{\mathrm{f,b}}^{\mathrm{eff}}\nabla_{\boldsymbol{R}}\rho_\mathrm{s}(\boldsymbol{R})$, with $\mu_{\mathrm{f,b}}^{\mathrm{eff}}$ given by (21). The subscripts f and b imply that the separation averages $\langle\cdot\rangle$ appearing in the definition of each quantity are performed using the interaction potentials corresponding to the free and bound state, respectively, which will in general be different from each other. We also note that the binding-induced velocity can be rewritten as $\mathbf{V}_{\mathrm{bi}}^{\mathrm{eff}}(\boldsymbol{R}) = -\nabla_{\boldsymbol{R}}D^{\mathrm{eff}}(\boldsymbol{R})$. In the absence of phoresis ($\mathbf{V}_{\mathrm{ph}}^{\mathrm{eff}} = 0$), Eq. (2) can be rewritten as $\partial_t c_\mathrm{tot}(\boldsymbol{R};t) = \nabla_{\boldsymbol{R}}^2\{D^{\mathrm{eff}}(\boldsymbol{R})c_\mathrm{tot}\}$, which shows that in the stationary state the enzyme tends to accumulate in regions where the diffusion coefficient is lowest,[13,23] with $c_\mathrm{tot}(\boldsymbol{R}) \propto 1/D^{\mathrm{eff}}(\boldsymbol{R})$.

The form of Eq. (2) depends on details of the enzymes' kinetics. We have focused on the case of rotational diffusion being faster than the mean binding time. If instead one assumes that the binding rate is much faster than rotational diffusion, the hydrodynamic

corrections in (31) and (33) will have different forms. Furthermore, $\mathbf{V}_{\rm bi}^{\rm eff}$ can no longer be written exactly as the derivative of the diffusion coefficient. Generically, any quantity that depends on the coupling between the fast (local) and slow (global) dynamics will be determined by this time-scale separation.

VI. CONCLUSIONS

The specific geometry of an asymmetric dumbbell was used to study the response of an enzyme to an inhomogeneous concentration of its substrate in order to access the hydrodynamic interactions that arise in the flexible, modular structure of an enzyme. The interactions of the enzyme with the substrate concentration gradient produces a drift velocity and a tendency to align parallel or anti-parallel to the gradient, depending on the sign of the interactions between the enzyme and substrate molecules. Specifically, the enzyme will typically orient so that the subunit that is most attracted to the substrate (or least repelled from the substrate, if both are repelled) is located in the region of higher substrate concentration. If both subunits have equal interactions with the substrate, the enzyme will reorient so that the larger subunit is in the region of higher or lower substrate concentration if the interactions are attractive or repulsive, respectively. We also find a second alignment mechanism, due to gradients in the concentration field of the *enzyme*, that is controlled by the strength of the coupling between the translational and rotational motion of the enzyme, and leads to reorientation so that the larger subunit is in the region of higher enzyme concentration. The effects of the two alignment mechanisms, particularly of alignment due to hydrodynamic interactions, and the non-linear coupling of the two are likely to be significant for the collective behaviour of many interacting enzymes. The predictions of Saha *et al.* on collective behaviour of chemotactic particles,[22] of Mikhailov *et al.* on collective hydrodynamics of active proteins,[27] and of Sweetlove *et al.* on possible mechanisms for structure formation by enzymes,[1] suggest that the subtle balance of translational and rotational coupling mediated by both hydrodynamic and chemical fields that we have uncovered here for a single enzyme should lead to self-organisation in dense enzyme solutions.

In previous work, we showed that the diffusion coefficient of a modular macromolecule is overestimated if it is considered as a rigid, symmetric object. Here, we have shown that the drift velocity in a substrate gradient is also modified for a flexible macromolecule. Though the form of the fluctuation-induced corrections we present is specific to the ordering of time-scales and hence to a chosen enzyme kinetics, the case we considered is the most relevant given that it corresponds to the ordering that is most observed in typical enzymes.

Finally, we note that our analysis and results can be easily generalised, for example to account for non-spherical subunits and include the orientational fluctuations that such subunits can undergo.[28]

ACKNOWLEDGMENTS

We thank Pierre Illien and Suropriya Saha for invaluable discussions. This work was supported by the U.S. National Science Foundation under MRSEC Grant No. DMR-1420620. T.A.L. acknowledges the support of an EPSRC Studentship.

APPENDIX A: INTEGRATION OF PHORETIC TERMS

1. Self-type phoretic terms

Integrals of the type

$$\int_X (\boldsymbol{\mu}^{is} - \boldsymbol{\mu}^{ii})(\mathrm{e}^{-\frac{\phi^{is}}{k_B T}} - 1)\nabla_X \rho_s \tag{A1}$$

are identical to those appearing in the case of phoresis of a single particle.[20,23]

For a spherical subunit i of radius a_i, assuming the substrate molecules are point-like, we have the mobility tensors

$$\boldsymbol{\mu}^{ii} = \frac{1}{6\pi\eta a_i}\mathbf{1} \tag{A2}$$

and

$$\boldsymbol{\mu}^{is} = \frac{1}{6\pi\eta a_i}\left[\frac{1}{4}\left(3\frac{a_i}{r_i} + \frac{a_i^3}{r_i^3}\right)\mathbf{1} + \frac{3}{4}\left(\frac{a_i}{r_i} - \frac{a_i^3}{r_i^3}\right)\hat{\boldsymbol{r}}_i\hat{\boldsymbol{r}}_i\right], \tag{A3}$$

where r_i is the distance between the center of subunit i and the substrate molecule, and $\hat{\boldsymbol{r}}_i$ is the radial unit vector. Combining both, we have

$$\boldsymbol{\mu}^{is} - \boldsymbol{\mu}^{ii} = \frac{1}{6\pi\eta a_i}\left[\left(-1 + \frac{3}{4}\frac{a_i}{r_i} + \frac{1}{4}\frac{a_i^3}{r_i^3}\right)(\mathbf{1} - \hat{\boldsymbol{r}}_i\hat{\boldsymbol{r}}_i) + \left(-1 + \frac{3}{2}\frac{a_i}{r_i} - \frac{1}{2}\frac{a_i^3}{r_i^3}\right)\hat{\boldsymbol{r}}_i\hat{\boldsymbol{r}}_i\right]. \tag{A4}$$

The concentration of substrate in the proximity of a subunit, assuming that far enough from the subunit there is a concentration gradient $\nabla\rho_s^\infty = |\nabla\rho_s^\infty|\hat{\boldsymbol{z}}$ of substrate molecules pointing in the z-direction, is given by the solution to the Laplace equation with no normal flux boundary conditions on the surface of the sphere

$$\rho_s(r_i, \theta_i, \varphi_i) = A + |\nabla\rho_s^\infty|\left(r_i + \frac{1}{2}\frac{a_i^3}{r_i^2}\right)\cos\theta_i, \tag{A5}$$

where we use spherical coordinates centred on the subunit i. Using the gradient operator in spherical coordinates $\nabla f = \partial_r f\hat{\boldsymbol{r}} + (1/r)\partial_\theta f\hat{\boldsymbol{\theta}} + (1/r\sin\theta)\partial_\varphi f\hat{\boldsymbol{\varphi}}$, we calculate

$$\nabla\rho_s = |\nabla\rho_s^\infty|\left[\left(1 - \frac{a_i^3}{r_i^3}\right)\cos\theta_i\hat{\boldsymbol{r}}_i - \left(1 + \frac{1}{2}\frac{a_i^3}{r_i^3}\right)\sin\theta_i\hat{\boldsymbol{\theta}}_i\right]. \tag{A6}$$

In order to evaluate (A1), we need

$$(\mathbf{1} - \hat{\boldsymbol{r}}_i\hat{\boldsymbol{r}}_i)\nabla\rho_s = -|\nabla\rho_s^\infty|\left(1 + \frac{1}{2}\frac{a_i^3}{r_i^3}\right)\sin\theta_i\hat{\boldsymbol{\theta}}_i \tag{A7}$$

and

$$(\hat{\boldsymbol{r}}_i\hat{\boldsymbol{r}}_i)\nabla\rho_s = |\nabla\rho_s^\infty|\left(1 - \frac{a_i^3}{r_i^3}\right)\cos\theta_i\hat{\boldsymbol{r}}_i. \tag{A8}$$

Furthermore, using the definition in Cartesian coordinates of $\hat{\boldsymbol{r}} = \sin\theta\cos\varphi\hat{\boldsymbol{x}} + \sin\theta\sin\varphi\hat{\boldsymbol{y}} + \cos\theta\hat{\boldsymbol{z}}$ and $\hat{\boldsymbol{\theta}} = \cos\theta\cos\varphi\hat{\boldsymbol{x}} + \cos\theta\sin\varphi\hat{\boldsymbol{y}} - \sin\theta\hat{\boldsymbol{z}}$, we can calculate the integrals over the solid angle $\int \mathrm{d}\Omega\sin\theta\hat{\boldsymbol{\theta}} = -(8\pi/3)\hat{\boldsymbol{z}}$ and $\int \mathrm{d}\Omega\cos\theta\hat{\boldsymbol{r}} = (4\pi/3)\hat{\boldsymbol{z}}$.

Taking together all these results, and noting that the two sets of coordinates used are related to each other by $\boldsymbol{X} = \boldsymbol{R} + r_i\hat{\boldsymbol{r}}_i$, we can finally evaluate (A1) to be

$$\int_X (\boldsymbol{\mu}^{is} - \boldsymbol{\mu}^{ii})(e^{-\frac{\phi^{is}}{k_B T}} - 1)\nabla_X \rho_s = -\frac{A_i}{\eta}\nabla_R \rho_s^\infty, \tag{A9}$$

where we have defined

$$A_i \equiv \frac{1}{6a_i}\int_{a_i}^\infty dr_i\, r_i^2\,(e^{-\frac{\phi^{is}}{k_B T}} - 1)\left(4 - 4\frac{a_i}{r_i} + \frac{a_i^4}{r_i^4} - \frac{a_i^6}{r_i^6}\right). \tag{A10}$$

For very short ranged interactions, we can use the approximation $r_i = a_i + \delta$ with $\delta \ll a_i$. The terms inside the rightmost parenthesis in the integral become $6\delta/a_i$ to lowest order, giving (11) from the main text.

2. Cross-type phoretic terms

We also need to evaluate integrals of the type

$$\int_X (\boldsymbol{\mu}^{is} - \boldsymbol{\mu}^{12})(e^{-\frac{\phi^{js}}{k_B T}} - 1)\nabla_X \rho_s, \tag{A11}$$

with $i \neq j$.

For spherical subunits of radius a_i and point-like substrate molecules, the mobility tensors are

$$\boldsymbol{\mu}^{is} = \frac{1}{6\pi\eta a_i}\left[\frac{1}{4}\left(3\frac{a_i}{r_i} + \frac{a_i^3}{r_i^3}\right)\mathbf{1} + \frac{3}{4}\left(\frac{a_i}{r_i} - \frac{a_i^3}{r_i^3}\right)\hat{\boldsymbol{r}}_i\hat{\boldsymbol{r}}_i\right] \tag{A12}$$

and

$$\boldsymbol{\mu}^{12} \simeq \frac{1}{8\pi\eta}\left[\left(\frac{1}{l} + \frac{a_1^2 + a_2^2}{3l^3}\right)\mathbf{1} + \left(\frac{1}{l} - \frac{a_1^2 + a_2^2}{l^3}\right)\hat{\boldsymbol{n}}\hat{\boldsymbol{n}}\right]. \tag{A13}$$

In order to evaluate (A11), we are interested in evaluating $\boldsymbol{\mu}^{2s}$ in the proximity of particle 1 and $\boldsymbol{\mu}^{1s}$ in the proximity of particle 2. Using the relation $\boldsymbol{r}_2 = \boldsymbol{r}_1 - \boldsymbol{l}$ and expanding in powers of r_1/l up to order $O(r_1^2/l^2) \sim O(a_1^2/l^2)$, which is of the same order as $\boldsymbol{\mu}$,[12] we can write $\boldsymbol{\mu}^{2s}$ as

$$\begin{aligned}\boldsymbol{\mu}^{2s} \simeq \frac{1}{8\pi\eta}\Bigg\{&\left[\frac{1}{l}\left(1 + \alpha_1\frac{r_1}{l} + \frac{1}{2}(3\alpha_1^2 - 1)\frac{r_1^2}{l^2}\right) + \frac{1}{3}\frac{a_2^2}{l^3}\right]\mathbf{1}\\ &+\left[\frac{1}{l}\left(1 + 3\alpha_1\frac{r_1}{l} + \frac{3}{2}(5\alpha_1^2 - 1)\frac{r_1^2}{l^2}\right) - \frac{a_2^2}{l^3}\right]\hat{\boldsymbol{n}}\hat{\boldsymbol{n}}\\ &-\frac{r_1}{l^2}\left[1 + 3\alpha_1\frac{r_1}{l}\right](\hat{\boldsymbol{r}}_1\hat{\boldsymbol{n}} + \hat{\boldsymbol{n}}\hat{\boldsymbol{r}}_1) + \frac{r_1^2}{l^3}\hat{\boldsymbol{r}}_1\hat{\boldsymbol{r}}_1\Bigg\},\end{aligned} \tag{A14}$$

with $\alpha_1 \equiv \hat{\boldsymbol{n}}\cdot\hat{\boldsymbol{r}}_i$. A similar expression can be obtained for $\boldsymbol{\mu}^{1s}$ in the proximity of particle 2, with

$$\begin{aligned}\boldsymbol{\mu}^{1s} \simeq \frac{1}{8\pi\eta}\Bigg\{&\left[\frac{1}{l}\left(1 - \alpha_2\frac{r_2}{l} + \frac{1}{2}(3\alpha_2^2 - 1)\frac{r_2^2}{l^2}\right) + \frac{1}{3}\frac{a_1^2}{l^3}\right]\mathbf{1}\\ &+\left[\frac{1}{l}\left(1 - 3\alpha_2\frac{r_2}{l} + \frac{3}{2}(5\alpha_2^2 - 1)\frac{r_2^2}{l^2}\right) - \frac{a_1^2}{l^3}\right]\hat{\boldsymbol{n}}\hat{\boldsymbol{n}}\\ &+\frac{r_2}{l^2}\left[1 - 3\alpha_2\frac{r_2}{l}\right](\hat{\boldsymbol{r}}_2\hat{\boldsymbol{n}} + \hat{\boldsymbol{n}}\hat{\boldsymbol{r}}_2) + \frac{r_2^2}{l^3}\hat{\boldsymbol{r}}_2\hat{\boldsymbol{r}}_2\Bigg\},\end{aligned} \tag{A15}$$

with $\alpha_2 \equiv \hat{\boldsymbol{n}}\cdot\hat{\boldsymbol{r}}_2$.

By considering the concentration of substrate centred around each subunit, and assuming that far from each subunit there is a concentration gradient $\nabla_R \rho_s^\infty = |\nabla_R \rho_s^\infty|\hat{z}$ of substrate molecules in the z-direction, the concentration gradient can be extracted from the integral in the same manner as for the self-type phoretic term above, giving

$$\int_X (\boldsymbol{\mu}^{is} - \boldsymbol{\mu}^{12})(e^{-\frac{\phi^{js}}{k_B T}} - 1)\nabla_X \rho_s = -\frac{a_j^3}{l^3}\frac{B_j}{\eta}\left(\hat{\boldsymbol{n}}\hat{\boldsymbol{n}} - \frac{\mathbf{1}}{3}\right)\nabla_R \rho_s^\infty, \tag{A16}$$

where we have defined

$$B_i \equiv \frac{1}{10}\int_{a_i}^\infty dr_i\, r_i\,(e^{-\frac{\phi^{is}}{k_B T}} - 1)\left(1 - 5\frac{r_i}{a_i} + 5\frac{r_i^3}{a_i^3}\right). \tag{A17}$$

In this case, considering very short ranged interactions we find (12).

3. Higher order corrections due to perturbation of solute concentration field by the other subunit

In the Appendixes A 1 and A 2, we have assumed that the concentration of substrate molecules around any given subunit is unaffected by the presence of the other subunit. Here, we show that this is not the case, and calculate the lowest order correction to the concentration field and its effect on the phoretic terms.

If we did a naive superposition of the fields around two particles of radii a_1 and a_2, we would write it as

$$\nabla\rho_s^{\text{naive}} = \nabla\rho_s^{(0)} + \nabla\rho_s^{(1)} + \nabla\rho_s^{(2)}, \tag{A18}$$

with

$$\begin{aligned}\nabla\rho_s^{(0)} &= |\nabla\rho_s^\infty|\left[\cos\theta_1\hat{\boldsymbol{r}}_1 - \sin\theta_1\hat{\boldsymbol{\theta}}_1\right]\\ &= |\nabla\rho_s^\infty|\left[\cos\theta_2\hat{\boldsymbol{r}}_2 - \sin\theta_2\hat{\boldsymbol{\theta}}_2\right] = |\nabla\rho_s^\infty|\hat{\boldsymbol{z}},\end{aligned} \tag{A19}$$

$$\begin{aligned}\nabla\rho_s^{(1)} &= -|\nabla\rho_s^\infty|\frac{a_1^3}{r_1^3}\left[\cos\theta_1\hat{\boldsymbol{r}}_1 + \frac{1}{2}\sin\theta_1\hat{\boldsymbol{\theta}}_1\right]\\ &= |\nabla\rho_s^\infty|\frac{a_1^3}{r_1^3}\left[-\hat{\boldsymbol{r}}_1\hat{\boldsymbol{r}}_1 + \frac{1}{2}\hat{\boldsymbol{\theta}}_1\hat{\boldsymbol{\theta}}_1\right]\hat{\boldsymbol{z}}\end{aligned} \tag{A20}$$

and

$$\begin{aligned}\nabla\rho_s^{(2)} &= -|\nabla\rho_s^\infty|\frac{a_2^3}{r_2^3}\left[\cos\theta_2\hat{\boldsymbol{r}}_2 + \frac{1}{2}\sin\theta_2\hat{\boldsymbol{\theta}}_2\right]\\ &= |\nabla\rho_s^\infty|\frac{a_2^3}{r_2^3}\left[-\hat{\boldsymbol{r}}_2\hat{\boldsymbol{r}}_2 + \frac{1}{2}\hat{\boldsymbol{\theta}}_2\hat{\boldsymbol{\theta}}_2\right]\hat{\boldsymbol{z}}\end{aligned} \tag{A21}$$

using Eq. (A6) for the solution around a single subunit, where $\hat{\boldsymbol{r}}_i, \hat{\boldsymbol{\theta}}_i$ are the unit vectors of spherical coordinates centred at the ith subunit, both sharing $\hat{\boldsymbol{z}}$ as the zenith direction. The two sets of coordinates are related by $r_1\hat{\boldsymbol{r}}_1 = l\hat{\boldsymbol{n}} + r_2\hat{\boldsymbol{r}}_2$.

The naive superposition is a solution of the Laplace equation, and it satisfies the boundary condition at infinity, but it does *not* satisfy the no normal flux boundary condition at the surface of the subunits. Indeed, the contribution $\nabla\rho_s^{(2)}$ in the proximity of subunit 1 is, to lowest order in $1/l$,

$$\begin{aligned}\nabla\rho_s^{(2)} &= \nabla\rho_s^{(2)}(r_1 = 0) + O\left(|\nabla\rho_s^\infty|\frac{a_2^3 r_1}{l^4}\right)\\ &= |\nabla\rho_s^\infty|\frac{3}{2}\frac{a_2^3}{l^3}\left[\frac{1}{3} - \hat{\boldsymbol{n}}\hat{\boldsymbol{n}}\right]\hat{\boldsymbol{z}} + O\left(|\nabla\rho_s^\infty|\frac{a_2^3 r_1}{l^4}\right),\end{aligned} \tag{A22}$$

where we have used the fact that at the center of subunit 1 we have $r_2 = l$, $\hat{\boldsymbol{r}}_2\hat{\boldsymbol{r}}_2 \cdot \hat{\boldsymbol{z}} = \hat{\boldsymbol{n}}\hat{\boldsymbol{n}} \cdot \hat{\boldsymbol{z}}$, and $\hat{\boldsymbol{\theta}}_2\hat{\boldsymbol{\theta}}_2 \cdot \hat{\boldsymbol{z}} = (\mathbf{1} - \hat{\boldsymbol{n}}\hat{\boldsymbol{n}}) \cdot \hat{\boldsymbol{z}}$. Therefore, to order $1/l^3$, the effect of the presence of subunit 2 is that it generates a uniform gradient around 1, that violates the no flux boundary condition. In order to cancel out this gradient while still satisfying the Laplace equation, we need to add a new term of the form

$$\nabla\rho_s^{(1,n)} = |\nabla\rho_s^{\infty}|\frac{3}{2}\frac{a_2^3}{l^3}\frac{a_1^3}{r_1^3}\left[-\hat{\boldsymbol{r}}_1\hat{\boldsymbol{r}}_1 + \frac{1}{2}\hat{\boldsymbol{\theta}}_1'\hat{\boldsymbol{\theta}}_1'\right]\left[\frac{\mathbf{1}}{3} - \hat{\boldsymbol{n}}\hat{\boldsymbol{n}}\right]\hat{\boldsymbol{z}}, \tag{A23}$$

where the unit vector $\hat{\boldsymbol{\theta}}_1'$ corresponds to spherical coordinates centred at subunit 1, but with the zenith direction parallel to $[\mathbf{1}/3 - \hat{\boldsymbol{n}}\hat{\boldsymbol{n}}]\hat{\boldsymbol{z}}$. It is easy to see that (A23) will cancel out the contribution of (A22) to the radial gradient at the surface of subunit 1 in the exact same way that (A20) cancels out the contribution of (A19). The same argument can be applied to the gradient generated by subunit 1 in the proximity of 2, resulting in a new term of the form

$$\nabla\rho_s^{(2,n)} = |\nabla\rho_0^{\infty}|\frac{3}{2}\frac{a_1^3}{l^3}\frac{a_2^3}{r_2^3}\left[-\hat{\boldsymbol{r}}_2\hat{\boldsymbol{r}}_2 + \frac{1}{2}\hat{\boldsymbol{\theta}}_2'\hat{\boldsymbol{\theta}}_2'\right]\left[\frac{\mathbf{1}}{3} - \hat{\boldsymbol{n}}\hat{\boldsymbol{n}}\right]\hat{\boldsymbol{z}}, \tag{A24}$$

where the unit vector $\hat{\boldsymbol{\theta}}_2'$ corresponds to spherical coordinates centred at subunit 2 with the zenith direction parallel to $[\mathbf{1}/3 - \hat{\boldsymbol{n}}\hat{\boldsymbol{n}}]\hat{\boldsymbol{z}}$.

All in all, the solute concentration gradient can therefore be written to order a_i^3/l^3 as

$$\nabla\rho_s \approx \nabla\rho_s^{(0)} + \nabla\rho_s^{(1)} + \nabla\rho_s^{(2)} + \nabla\rho_s^{(1,n)} + \nabla\rho_s^{(2,n)}. \tag{A25}$$

This expression satisfies exactly the Laplace equation and the boundary condition at infinity, and it also satisfies the no normal flux boundary conditions at the surface of the subunits up to order a_i^3/l^3.

The a_i^3/l^3 corrections to $\nabla\rho_s$ just described have an effect on the A-type contributions to the phoretic velocity. The integral (A9) picks up a correction, becoming

$$\int_X\left(\boldsymbol{\mu}^{is} - \boldsymbol{\mu}^{ii}\right)\cdot\left(\mathrm{e}^{-\frac{\phi^{is}}{k_BT}} - 1\right)\nabla_X\rho_s = -\frac{A_i}{\eta}\left[1 + \frac{3}{2}\frac{a_j^3}{l^3}\left(\frac{\mathbf{1}}{3} - \hat{\boldsymbol{n}}\hat{\boldsymbol{n}}\right)\right]\nabla_{\boldsymbol{R}}\rho_s^{\infty}. \tag{A26}$$

The B-type contribution (A16) is however unchanged to order a_i^3/l^3 because the corresponding corrections would be of order a_i^6/l^6.

APPENDIX B: AVERAGING OVER SEPARATION

There are two ways in which one can decompose gradients and divergences of the form $\nabla_{\boldsymbol{l}}A$ and $\nabla_{\boldsymbol{l}}\cdot\boldsymbol{A}$ into separation and orientation parts. One way is to use the orientational part of the $\nabla_{\boldsymbol{l}}$ operator $\tilde{\boldsymbol{\mathcal{R}}} = \partial/\partial\hat{\boldsymbol{n}} = l(\mathbf{1} - \hat{\boldsymbol{n}}\hat{\boldsymbol{n}})\nabla_{\boldsymbol{l}}$, in which case we have

$$\nabla_{\boldsymbol{l}}A = \frac{\partial A}{\partial l}\hat{\boldsymbol{n}} + \frac{1}{l}\tilde{\boldsymbol{\mathcal{R}}}A, \tag{B1}$$

with

$$\tilde{\boldsymbol{\mathcal{R}}}A = \frac{\partial A}{\partial\hat{\boldsymbol{n}}} = \frac{\partial A}{\partial\theta}\hat{\boldsymbol{\theta}} + \frac{1}{\sin\theta}\frac{\partial A}{\partial\varphi}\hat{\boldsymbol{\varphi}}, \tag{B2}$$

as well as

$$\nabla_{\boldsymbol{l}}\cdot\boldsymbol{A} = \frac{1}{l^2}\frac{\partial(l^2\boldsymbol{A}\cdot\hat{\boldsymbol{n}})}{\partial l} + \frac{1}{l}\tilde{\boldsymbol{\mathcal{R}}}\cdot\boldsymbol{A}, \tag{B3}$$

with

$$\tilde{\boldsymbol{\mathcal{R}}}\cdot\boldsymbol{A} = \frac{\partial}{\partial\hat{\boldsymbol{n}}}\cdot\boldsymbol{A} = \frac{1}{\sin\theta}\frac{\partial(\sin\theta\boldsymbol{A}\cdot\hat{\boldsymbol{\theta}})}{\partial\theta} + \frac{1}{\sin\theta}\frac{\partial(\boldsymbol{A}\cdot\hat{\boldsymbol{\varphi}})}{\partial\varphi}. \tag{B4}$$

Alternatively, one can use the angular momentum operator $\boldsymbol{\mathcal{R}} = \hat{\boldsymbol{n}}\times\partial/\partial\hat{\boldsymbol{n}}$, which satisfies the identities

$$\begin{aligned}\tilde{\boldsymbol{\mathcal{R}}}A &= -\hat{\boldsymbol{n}}\times(\boldsymbol{\mathcal{R}}A),\\ \tilde{\boldsymbol{\mathcal{R}}}\cdot\boldsymbol{A} &= \boldsymbol{\mathcal{R}}\cdot(\hat{\boldsymbol{n}}\times\boldsymbol{A}),\\ \tilde{\boldsymbol{\mathcal{R}}}\cdot(\tilde{\boldsymbol{\mathcal{R}}}A) &= \boldsymbol{\mathcal{R}}\cdot(\boldsymbol{\mathcal{R}}A).\end{aligned} \tag{B5}$$

The Smoluchowski equation (7) can be decomposed in this way to give

$$\begin{aligned}\partial_t\rho_e(\boldsymbol{R},\hat{\boldsymbol{n}},l;t) = {}& \frac{1}{4}\nabla_{\boldsymbol{R}}\cdot(k_BT\mathbf{M}\cdot\nabla_{\boldsymbol{R}}\rho_e) + \tilde{\boldsymbol{\mathcal{R}}}\cdot\left(k_BT\frac{W_I}{l^2}\tilde{\boldsymbol{\mathcal{R}}}\rho_e\right) + \frac{1}{2}\tilde{\boldsymbol{\mathcal{R}}}\cdot\left(k_BT\frac{\Gamma_I}{l}\nabla_{\boldsymbol{R}}\rho_e\right)\\ &+ \frac{1}{2}\nabla_{\boldsymbol{R}}\cdot\left(k_BT\frac{\Gamma_I}{l}\tilde{\boldsymbol{\mathcal{R}}}\rho_e\right) + \frac{1}{2}\nabla_{\boldsymbol{R}}\cdot\left[(\Gamma_I+\Gamma_D)\left(k_BT\frac{\partial\rho_e}{\partial l} + U'\rho_e\right)\hat{\boldsymbol{n}}\right]\\ &+ \frac{1}{2}\frac{1}{l^2}\frac{\partial}{\partial l}\left[l^2k_BT(\Gamma_I+\Gamma_D)\hat{\boldsymbol{n}}\cdot\nabla_{\boldsymbol{R}}\rho_e\right] + \frac{1}{l^2}\frac{\partial}{\partial l}\left[l^2(W_I+W_D)\left(k_BT\frac{\partial\rho_e}{\partial l} + U'\rho_e\right)\right]\\ &- \nabla_{\boldsymbol{R}}\cdot\left\{\frac{k_BT}{2\eta}\rho_e\left[A_1 + A_2 + \frac{1}{l^3}\left(a_1^3B_1 + a_2^3B_2 - \frac{3}{2}(a_2^3A_1 + a_1^3A_2)\right)\left(\hat{\boldsymbol{n}}\hat{\boldsymbol{n}} - \frac{\mathbf{1}}{3}\right)\right]\cdot\nabla_{\boldsymbol{R}}\rho_s^{\infty}\right\}\\ &- \tilde{\boldsymbol{\mathcal{R}}}\cdot\left\{\frac{k_BT}{\eta}\rho_e\left[\frac{A_2 - A_1}{l} + \frac{1}{3}\frac{1}{l^4}\left(a_2^3B_2 - a_1^3B_1 + \frac{3}{2}(a_1^3A_2 - a_2^3A_1)\right)\right]\nabla_{\boldsymbol{R}}\rho_s^{\infty}\right\}\\ &- \frac{1}{l^2}\frac{\partial}{\partial l}\left\{l^2\rho_e[(\boldsymbol{\sigma}_2 - \boldsymbol{\sigma}_1)\cdot\nabla_{\boldsymbol{R}}\rho_s^{\infty}]\cdot\hat{\boldsymbol{n}}\right\},\end{aligned} \tag{B6}$$

which after performing the separation averaging and using the identities (B5), can be rewritten as

$$\partial_t\tilde{\rho}_e(\boldsymbol{R},\hat{\boldsymbol{n}};t) = \frac{1}{4}\nabla_{\boldsymbol{R}}\cdot(k_BT\langle\mathbf{M}\rangle\cdot\nabla_{\boldsymbol{R}}\tilde{\rho}_e) + \boldsymbol{\mathcal{R}}\cdot\left(k_BT\left\langle\frac{W_I}{l^2}\right\rangle\boldsymbol{\mathcal{R}}\tilde{\rho}_e\right) + \frac{1}{2}\boldsymbol{\mathcal{R}}\cdot\left(k_BT\left\langle\frac{\Gamma_I}{l}\right\rangle(\hat{\boldsymbol{n}}\times\nabla_{\boldsymbol{R}}\tilde{\rho}_e)\right) - \frac{1}{2}\nabla_{\boldsymbol{R}}\cdot\left(k_BT\left\langle\frac{\Gamma_I}{l}\right\rangle(\hat{\boldsymbol{n}}\times\boldsymbol{\mathcal{R}}\tilde{\rho}_e)\right)$$
$$-\nabla_{\boldsymbol{R}}\cdot\left\{\frac{k_BT}{2\eta}\tilde{\rho}_e\left[A_1+A_2+\left\langle\frac{1}{l^3}\right\rangle\left(a_1^3B_1+a_2^3B_2-\frac{3}{2}(a_2^3A_1+a_1^3A_2)\right)\left(\hat{\boldsymbol{n}}\hat{\boldsymbol{n}}-\frac{\mathbf{1}}{3}\right)\right]\cdot\nabla_{\boldsymbol{R}}\rho_s^{\infty}\right\}$$
$$-\boldsymbol{\mathcal{R}}\cdot\left\{\frac{k_BT}{\eta}\tilde{\rho}_e\left[\left\langle\frac{1}{l}\right\rangle(A_2-A_1)+\frac{1}{3}\left\langle\frac{1}{l^4}\right\rangle\left(a_2^3B_2-a_1^3B_1+\frac{3}{2}(a_1^3A_2-a_2^3A_1)\right)\right](\hat{\boldsymbol{n}}\times\nabla_{\boldsymbol{R}}\rho_s^{\infty})\right\}, \tag{B7}$$

from which Eq. (1) follows.

REFERENCES

[1] L. J. Sweetlove and A. R. Fernie, Nat. Commun. **9** (2018).
[2] F. Wu, L. N. Pelster, and S. D. Minteer, Chem. Commun. **51**, 1244 (2015).
[3] S. Sengupta, K. K. Dey, H. S. Muddana, T. Tabouillot, M. E. Ibele, P. J. Butler, and A. Sen, J. Am. Chem. Soc. **135**, 1406 (2013).
[4] K. K. Dey, X. Zhao, B. M. Tansi, W. J. Méndez-Ortiz, U. M. Córdova-Figueroa, R. Golestanian, and A. Sen, Nano Lett. **15**, 8311 (2015).
[5] P. Illien, R. Golestanian, and A. Sen, Chem. Soc. Rev. **46**, 5508 (2017).
[6] H. Yu, K. Jo, K. L. Kounovsky, J. J. d. Pablo, and D. C. Schwartz, J. Am. Chem. Soc. **131**, 5722 (2009).
[7] H. S. Muddana, S. Sengupta, T. E. Mallouk, A. Sen, and P. J. Butler, J. Am. Chem. Soc. **132**, 2110 (2010).
[8] S. Sengupta, M. M. Spiering, K. K. Dey, W. Duan, D. Patra, P. J. Butler, R. D. Astumian, S. J. Benkovic, and A. Sen, ACS Nano **8**, 2410 (2014).
[9] C. Riedel, R. Gabizon, C. A. M. Wilson, K. Hamadani, K. Tsekouras, S. Marqusee, S. Press, and C. Bustamante, Nature **517**, 227 (2015).
[10] P. Illien, X. Zhao, K. K. Dey, P. J. Butler, A. Sen, and R. Golestanian, Nano Lett. **17**, 4415 (2017).
[11] K. K. Dey, S. Das, M. F. Poyton, S. Sengupta, P. J. Butler, P. S. Cremer, and A. Sen, ACS Nano **8**, 11941 (2014).
[12] X. Zhao, H. Palacci, V. Yadav, M. M. Spiering, M. K. Gilson, P. J. Butler, H. Hess, S. J. Benkovic, and A. Sen, Nat. Chem. **10**, 311–317 (2018).
[13] A.-Y. Jee, S. Dutta, Y.-K. Cho, T. Tlusty, and S. Granick, Proc. Natl. Acad. Sci. U. S. A. **115**, 14 (2018).
[14] J. Agudo-Canalejo, T. Adeleke-Larodo, P. Illien, and R. Golestanian, Acc. Chem. Res. **51**, 2365 (2018).
[15] R. Golestanian, Phys. Rev. Lett. **105**, 018103 (2010).
[16] R. Golestanian, Phys. Rev. Lett. **115**, 108102 (2015).
[17] X. Bai and P. G. Wolynes, J. Chem. Phys. **143**, 165101 (2015).
[18] W. Hwang and C. Hyeon, J. Phys. Chem. Lett. **8**, 250 (2017).
[19] P. Illien, T. Adeleke-Larodo, and R. Golestanian, Europhys. Lett. **119**, 40002 (2017).
[20] J. L. Anderson, Annu. Rev. Fluid. Mech. **21**, 61 (1989).
[21] H. A. Stone and A. D. T. Samuel, Phys. Rev. Lett. **77**, 4102 (1996).
[22] S. Saha, R. Golestanian, and S. Ramaswamy, Phys. Rev. E **89**, 062316 (2014).
[23] J. Agudo-Canalejo, P. Illien, and R. Golestanian, Nano Lett. **18**, 2711 (2018).
[24] S. Lee and M. Karplus, J. Chem. Phys. **86**, 1883 (1987).
[25] B. V. Derjaguin, G. P. Sidorenkov, E. A. Zubashchenko, and E. V. Kiseleva, Kolloidn. Zh. **9**, 335–347 (1947).
[26] S. Ebbens, M.-H. Tu, J. R. Howse, and R. Golestanian, Phys. Rev. E **85**, 020401 (2012).
[27] A. S. Mikhailov and R. Kapral, Proc. Natl. Acad. Sci. U. S. A. **112**, E3639 (2015).
[28] T. Adeleke-Larodo, P. Illien, and R. Golestanian, "Fluctuation-induced hydrodynamic coupling in an asymmetric, anisotropic dumbbell," Eur. Phys. J. E (to be published); eprint arXiv:1712.06418 (2017).